Hindawi
Mathematical Problems in Engineering
Volume 2020, Article ID 6730284, 7 pages
https://doi.org/10.1155/2020/6730284

Research Article

A Power Factor Correction Buck Converter-Fed Switched Reluctance Motor with Torque Ripple Suppression

Jianli Jing

School of Electronic and Electrical Engineering, Bengbu University, Bengbu 233030, China

Correspondence should be addressed to Jianli Jing; jingjl98@163.com

Received 23 March 2020; Revised 7 June 2020; Accepted 11 June 2020; Published 13 July 2020

Academic Editor: Andras Szekrenyes

The switched reluctance motor (SRM) suffers the main drawback of torque ripples, and a buck converter-fed SRM motor drive has been proposed to suppress torque ripples and correct a power factor in this paper. The buck converter reduces the torque ripple by supplying appropriate DC-link voltage; meanwhile, the buck converter realizes a function of power factor correction at AC mains. An enhanced performance has been obtained on speed control and power quality improvement. An experimental SRM motor drive is formed, and the experimental results show that the proposed drive possesses an improved function with suppression of torque ripples and power factor correction.

1. Introduction

Due to low cost, simple structure, fault tolerance, and good controllability, the switched reluctance motor is widely used in industrial applications as a variable speed drive, particularly in high-speed applications [1–3]. However, the switched reluctance motor suffers from torque ripples, which results in the vibration and noise, restricts its application to a high-performance servo system [4, 5, 8].

The method of torque ripple suppression for the SRM mainly includes optimization of switching angle [9, 10], direct torque control [11, 12], torque-sharing function [13, 14], intelligent control [15–17], and variable DC-link voltage [18, 19, 22]. The method of switching angle optimization is usually applicative in small range, and the algorithm of direct torque control, torque-sharing function, and intelligent control is complex.

In [23], an active boost converter with a capacitance and an insulated gate bipolar transistor is presented to control the excitation voltage and demagnetization voltage applied to the SRM phases in real time, which can avoid negative torque of the demagnetization phase by controlling the commutation time accurately and reduce the torque ripple effectually in a commutation interval.

In [24], a DC chopper between the rectifier and the power converter of the switched reluctance motor in order to control the DC-link voltage is presented, where the DC-link voltage changes with speed, and in the entire speed range, the motor always operates in the single pulse state. Such a control scheme reduces the current gradient and the acoustic noise, and extends the life expectancy of the motor.

The authors in [23, 24] reduce the torque ripple of the SRM preferably by adjusting the DC-link voltage, but power factor correction (PFC) is not considered. The conventional SRM drive is normally supplied by a diode bridge rectifier and a large DC-link capacitor, the diode bridge rectifier draws a pulse current from the AC mains, the accompanying harmonics will exceed the restricts given in the standards [25]. The power supply of SRM drive without power factor correction function leads to harmonic pollution, poor factor, and low efficiency. Hence, the active power factor correction converter is introduced in SRM drive for improving the power quality at AC mains.

In [26], a modified quasi Z-source converter in front of an asymmetric half-bridge converter for the switched reluctance motor is proposed, the quasi Z-source converter not only improves the speed regulation performance of the drive system and reduces the torque ripple by adjusting DC bus voltage according to the operation condition but also

reduces total harmonic distortion and improves the power factor by the peak current control.

In [27], a power factor correction converter composed by two cuk circuits with a communal switch fed switched reluctance motor is proposed, the modified cuk converter reduces torque ripples by adjusting DC bus voltage according to speed, and at the same time, it improved the power factor in wide speed range.

The authors of [26, 27] reduce the torque ripples of the SRM and increase the power factor preferably through the DC converter, but its structure and implementation is relatively complicated. A fine solution for torque ripple suppression of the SRM is to feed the motor with low voltage in the low speed range and to increase voltage accordingly when the speed increases.

A novel simple buck power converter with power factor correction for the SRM is presented in this paper, it not only can control the DC-link voltage to reduce the torque ripple in wide speed range but also can significantly improve the power quality at AC mains, and it does not require a complex algorithm compared with the other control strategies.

2. Analysis of Torque Ripple

The doubly salient switched reluctance motor has independent phase windings on the stator, and the phase voltage equation is given by

$$U = Ri + L\frac{di}{dt} + i\frac{dL}{dt}, \tag{1}$$

where U is the phase voltage, R is the resistance of phase winding, i is the phase current, and L is the phase inductance relying on the rotor position and the phase current.

The phase back electromotive force (EMF) E is given by

$$E = i\frac{dL}{dt} = i\frac{dL}{d\theta}\frac{d\theta}{dt} = i\omega\frac{dL}{d\theta}, \tag{2}$$

where θ and ω represent the rotor angular position and the rotor velocity, respectively.

So, the phase voltage equation can be written as

$$U = Ri + L\frac{di}{dt} + E. \tag{3}$$

Assuming the magnetism is linear, the phase torque can be given by [5]

$$T = \frac{1}{2}i^2\frac{dL}{d\theta} = \frac{1}{2}i^2K, \tag{4}$$

where K denotes the change rate of phase inductance with angle.

From equation (4), it can be seen that the torque is proportionate to the square of current. K is a function of the phase-winding current and rotor position in reality, but usually, its variation is much smaller than that in current squared, [28] so the torque stability is mainly determined by the current stability. In a steady state, neglecting the resistance drop, from equation (4), it can be implied that if the phase voltage is equal to the phase back electromotive force, the current will be constant, so the torque will be constant. Since the phase back electromotive force is proportionate to the rotor velocity, the desired voltage of the inverter for SRM drive should vary with the rotor velocity and the desired voltage of the inverter for SRM drive should approximately proportional to the rotor velocity, and then the torque will be smooth.

The most commonly used method for the switched reluctance motor is current chopping control, particularly at low-speed and start-up area. The block diagram of the current chopping control for the switched reluctance motor is shown in Figure 1. Due to doubly salient poles and centralized field excitation, the switched reluctance motor is inclined to considerable vibration and acoustic noise. The vibration and noise is particularly notable at low-speed and start-up area in the current chopping control method.

The vibration of SRM is caused by the variation of the radial force, and the variation of the radial force is caused by the change of the voltage added to the winding, so the source of the vibration is the change of the voltage.

In the common control method, the voltage added to the winding is full DC-link voltage throughout the entire speed area and the voltage change gradient is maximal, so the vibration and attendant noise is maximal. Moreover, current normally exceeds the hysteresis width in practice, which leads to the larger current ripple along with the larger torque ripple [29].

3. Buck Converter for SRM

The configuration of the buck converter for the SRM is shown in Figure 2.

The buck converter is placed between the diode bridge rectifier and the inverter circuit of the SRM, the output voltage of the diode bridge rectifier is the input voltage of the buck converter, and the output voltage of the buck converter is the input voltage of the inverter circuit of the SRM. The relationship between input voltage and output voltage of the buck converter is indicated by the following equation:

$$V_{\mathrm{OUT}} = D \cdot V_{\mathrm{IN}}, \tag{5}$$

where V_{OUT} and V_{IN} represent the output voltage and input voltage, respectively, and D denotes the duty cycle of the switch.

A diode bridge rectifier with a capacitor usually results in the low power factor due to a pulsed input current which is far from the sinusoidal wave. A buck converter not only can convert the high input voltage to a low output voltage but also can correct the power factor by shaping the AC input current in the phase with the AC input voltage.

When the input voltage is higher than the output voltage and the power switch T is on, the input current is equal to the current of the inductor, energy from the AC mains is stored in the inductor L, while the power switch T is off, the input current becomes zero, and the inductor energy is transferred to the capacitor C. Figure 3 shows the block diagram of the buck PFC converter control, V_{IN} is a positive sinusoidal full wave rectified by the diode rectifier bridge, V_{OUT} is the DC

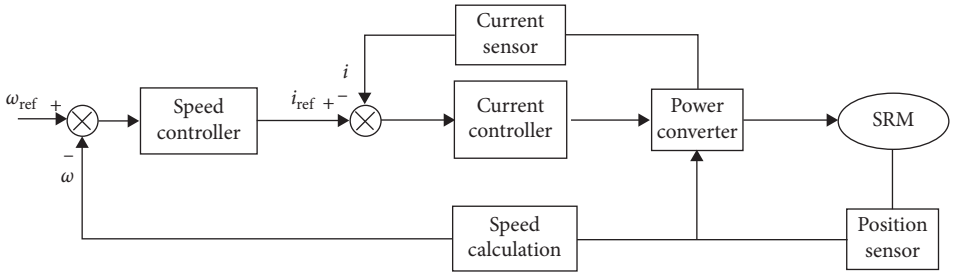

Figure 1: The block diagram of the current chopping control for SRM.

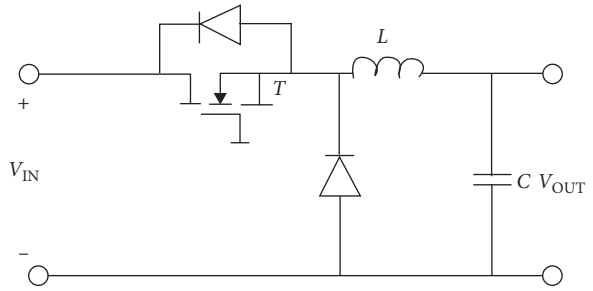

Figure 2: The configuration of the buck converter for the SRM.

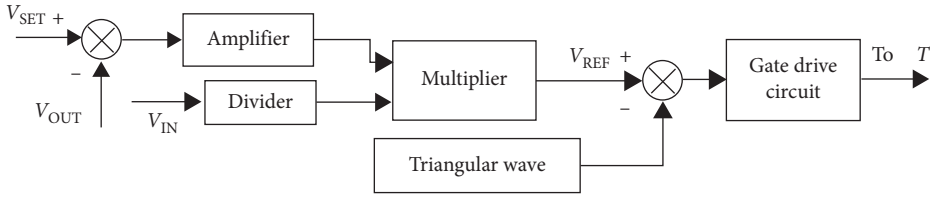

Figure 3: The block diagram of the buck PFC converter control.

output voltage of the buck converter, and V_{SET} is the setting DC output voltage of the buck converter. The difference between V_{SET} and V_{OUT} is amplified, V_{IN} is divided, the processed results are input to the multiplier, and V_{REF} is the output of the multiplier, so V_{REF} is a rectified sinusoidal wave whose amplitude is controlled by the output voltage of the buck converter. V_{REF} is compared to the triangular wave, and thus, the PWM wave driving the switching device T is generated, which shapes input current into a sinusoidal waveform in order to be in phase with the utility grid input voltage. The common pulse width modulation technique used in the buck converter usually results in a distortion in the AC input current due to the current ripple of the inductor, and the pulse area modulation technique is an improved control strategy for the buck PFC converter for reducing the harmonic current, which shapes the input current into a sinusoidal waveform by modulating the area of the current pulse [30].

When the current fluctuation in the inductor can be negligible, the input current wave of the buck PFC converter is shown in Figure 4, wave V_{REF} is a rectified sinusoidal wave so as to be in phase with the grid input voltage, and it is compared with the isosceles triangle waveform V_{car}; the comparison result determines the input current conduction time, and the input current I_{IN} is a sine sequence of pulses.

Figure 5 shows the schematic diagram of input current conduction time, the sinusoidal reference wave intersects a triangular carrier at E point, the line segment AB is a horizontal line, T is the period of the triangular wave, and t_{ON} is the input current conduction time of the buck PFC converter in a cycle. Equation (6) can be obtained from Figure 5:

$$\frac{m \cdot \sin \omega t_E}{t_{ON}/2} = \frac{1}{T/2}, \tag{6}$$

where m denotes modulation degree of the sine wave and ω denotes angular frequency of the sine wave. Equation (7) can be derived from equation (6):

$$t_{ON} = T \cdot m \cdot \sin \omega t_E. \tag{7}$$

From the above equation, it can be concluded that the input average current of the buck PFC converter is in proportional to the grid sinusoidal input voltage, and it will be a relatively good sine wave when its high-frequency harmonic components are eliminated with a small filter.

4. The Proposed Control Strategy for SRM

The full DC voltage leads to high current gradient and then motivates larger torque ripples and larger vibration along

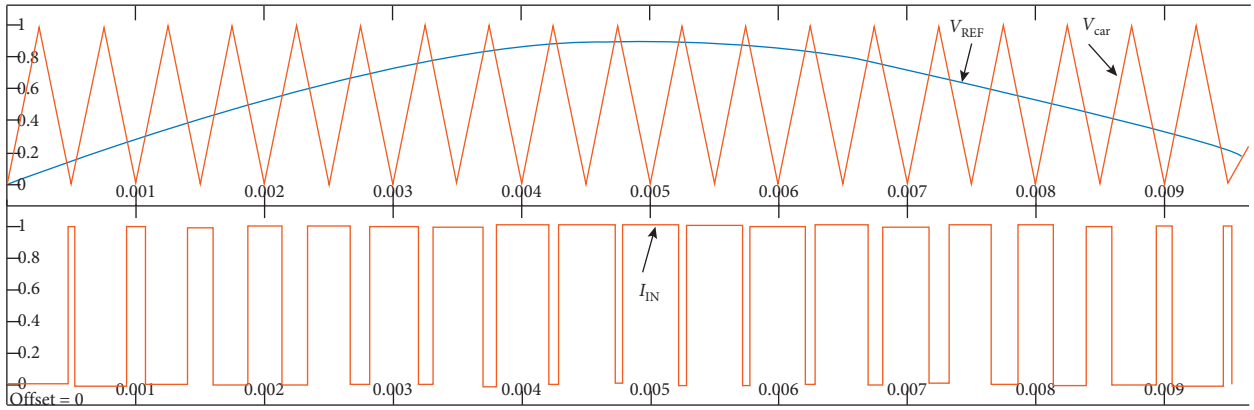

Figure 4: The input current wave of the buck PFC converter.

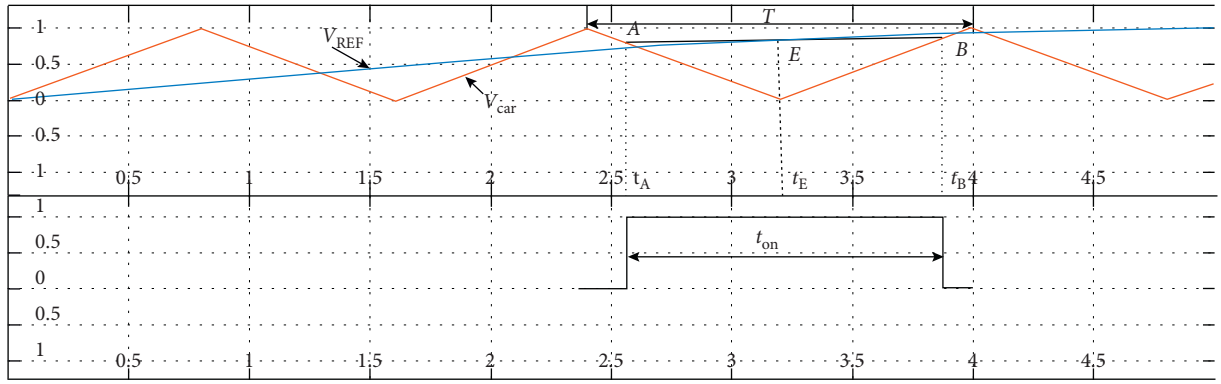

Figure 5: The schematic diagram of input current conduction time.

with acoustic noise. Because vibration amplitude is proportional to the rate of voltage change at the step change moment, the torque ripple is also related to the rate of voltage change at the step moment, so the torque ripple and vibration can be suppressed by decreasing the rate of voltage change, and the reduced DC-link voltage leads to reduced current gradient and thus the torque ripple compared with the traditional control method [31–33].

In the proposed control strategy, the DC bus voltage is controlled as a function of speed. The buck converter before the power converter outputs the suitable voltage for the switched reluctance motor, and the current of the winding will become smooth. The block diagram of the SRM drive with the buck converter is shown in Figure 6. The rotor position is fed back by the position sensor to the controller, the rotor speed is controlled in the outer control loop, the current is controlled in the inner loop, the error of speed generates the current command, and the error of current generates the switching signals of the power converter. The rotor speed generates the output voltage command to the buck converter.

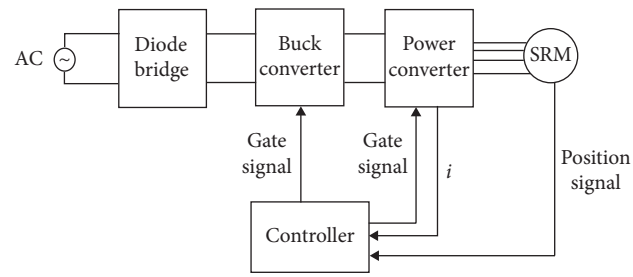

Figure 6: The block diagram of the SRM drive with the buck converter.

5. Experimental Result

To verify the availability of the proposed method, a four-phase 8/6 poles 75 W switched reluctance motor drive system with the buck converter is set up and a TMS320F2812 type DSP is employed for digital implementation of the control algorithm.

Figure 7 compares the speed waveforms without and with the buck converter at 300 r/min, and the rated speed of motor is 1500 r/min. As shown in the figure, the speed ripple of the drive with the buck converter is lower than that of the drive without the buck converter, and it implies the torque ripple is suppressed availably with the buck converter.

Figure 8 compares the current waveforms without and with the buck converter at 300 r/min, as shown in the figure; the current waveform of the drive with the buck converter is

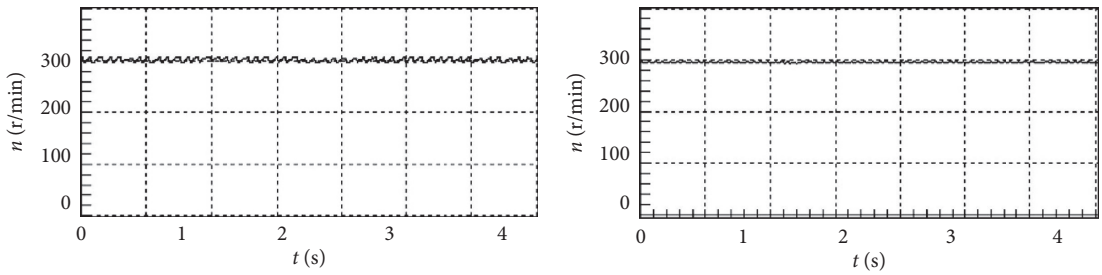

Figure 7: The speed waveform at 300 r/min: (a) without the buck converter; (b) with the buck converter.

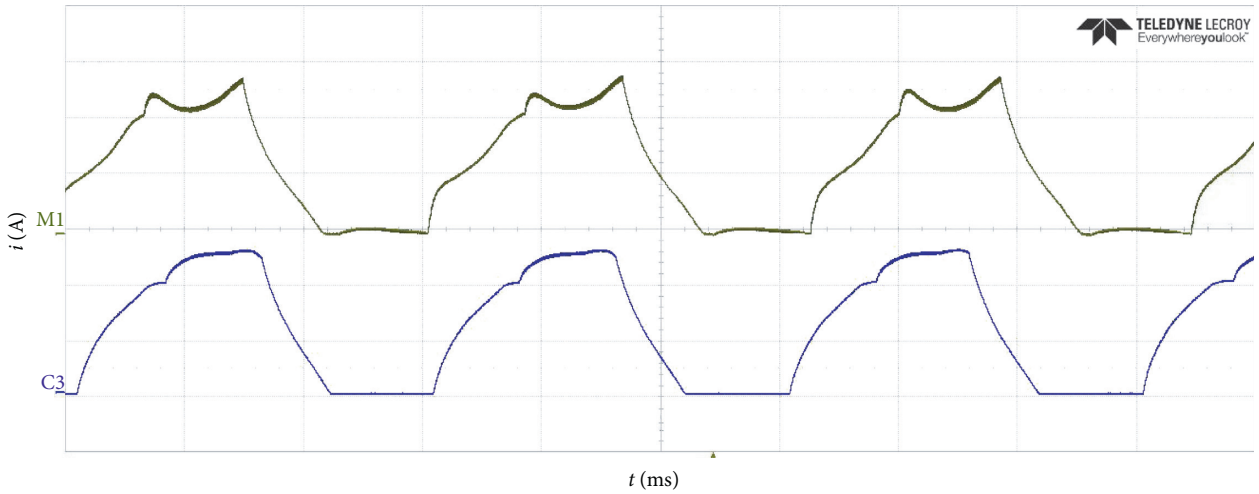

Figure 8: The current waveform at 300 r/min: up, without the buck converter; down, with the buck converter.

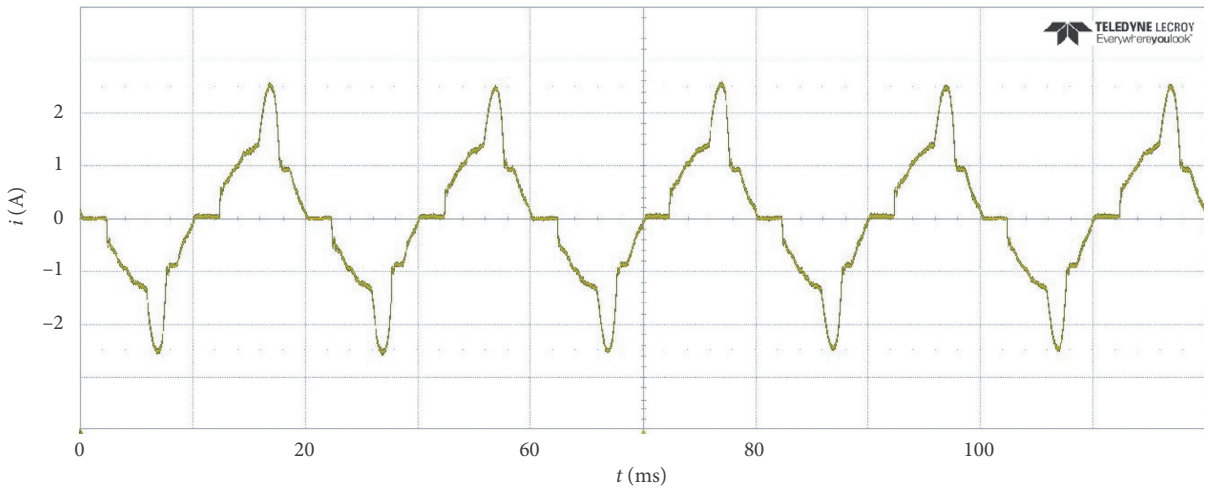

(a)

Figure 9: Continued.

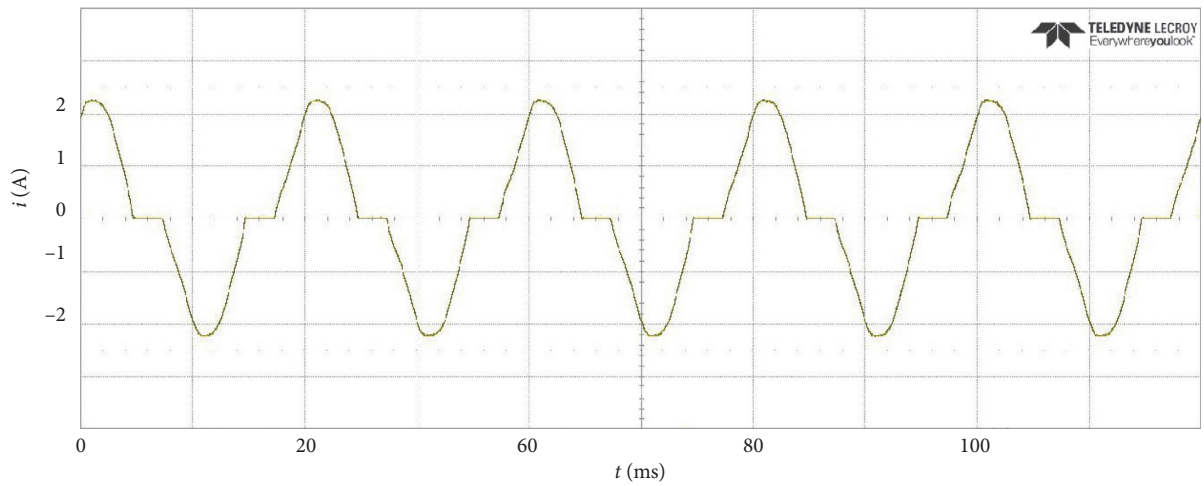

(b)

Figure 9: The input current waveform of the buck converter at 300 r/min: (a) without the buck converter; (b) with the buck converter.

smoother than that of the drive without the buck converter, and it implies that the torque is smoother.

The power factor is the ratio of active power to apparent power, and it consists of the displacement power factor and distortion power factor under the condition that the current waveform is nonsinusoidal. The displacement power factor is the ratio of the fundamental active power to the fundamental apparent power and is often denoted as the cosine of the phase angle between the fundamental voltage wave and fundamental current wave. The distortion power factor is related to harmonic content in current and is equal to the ratio between the root mean square (rms) value of the fundamental current and the root mean square value of the total current. The power factor (PF) can be represented as

$$\mathrm{PF} = \cos\theta \cdot \frac{I_1}{I_T} = \cos\theta \cdot \frac{1}{\sqrt{1 + THD}}, \tag{8}$$

where I_1 and I_T represent the rms value of fundamental current and total current, respectively, θ denotes the phase angle between fundamental voltage and current, and THD represents total harmonic distortion, equal to the ratio of the rms value of the total harmonic component to the rms value of the fundamental component.

Figure 9 shows the input current waveform of the buck converter at 300 r/min, it can be seen that the current waveform is closer to the sinusoidal waveform compared with the diode bridge rectifier, and it has less harmonic content; from equation (8), it implies that the property of power factor is enhanced.

6. Conclusion

A power factor corrected buck converter fed SRM motor drive has been proposed to suppress torque ripples in this paper. The buck converter supplies the desired voltage for SRM drive by controlling the voltage at DC bus and making it vary directly with the motor speed; accordingly, the torque ripple is suppressed. Meanwhile, the front-end buck converter realizes a function of power factor correction at AC mains. An enhanced performance has been obtained on speed control and improvement of power quality at AC mains. Finally, an experimental SRM motor drive is formed to validate the proposed drive, and the results of experiment verify the effectiveness of the proposed drive.

Data Availability

All data, models, or codes generated or used during the study are available from the corresponding author upon request.

Conflicts of Interest

The authors declare that they have no conflicts of interest.

Acknowledgments

This work was supported by the Young and Middle-Aged Excellent Teacher Foundation of Bengbu College, Natural Science Research Key Project of Bengbu University (2018ZR02zd), University Outstanding Youth Talent Spport Scheme (gxyq2019103), Anhui Province Quality Engineering Project (2016jyxm0392), and Quality Engineering Project of Bengbu University (2016JYXM11).

References

[1] M. Rajesh and B. Singh, "Analysis, design and control of single-phase three-level power factor correction rectifier fed switched reluctance motor drive," *IET Power Electronics*, vol. 7, no. 6, pp. 1499–1508, 2014.

[2] H. C. Chang and C. M. Liaw, "Development of a compact switched-reluctance motor drive for EV propulsion with voltage-boosting and PFC charging capabilities," *IEEE Transactions on Vehicular Technology*, vol. 58, p. 3198, 2009.

[3] T. H. Pham, "Design and control of a high speed 2-phase 4/2 switched reluctance motor for blender application," *Journal of Electrical Engineering and Technology*, vol. 14, p. 1193, 2019.

[4] X. Guo, R. Zhong, M. Zhang, D. Ding, and W. Sun, "Resonance reduction by optimal switch angle selection in switched reluctance motor," *IEEE Transactions on Industrial Electronics*, vol. 67, no. 3, pp. 1867–1877, 2020.

[5] V. Payam, "Multi-layer switched reluctance motors: performance prediction and torque ripple reduction," *International Transactions on Electrical Energy Systems*, vol. 30, no. 2, 2020.

[6] R. P. Krishna, "Direct torque and flux control of switched reluctance motor with enhanced torque per ampere ratio and torque ripple reduction," *Electronics Letters*, vol. 55, p. 477, 2019.

[7] A. Rashidi, S. M. Saghaiannejad, and S. J. Mousavi, "Acoustic noise reduction and power factor correction in switched reluctance motor drives," *Journal of Power Electronics*, vol. 11, no. 1, pp. 37–44, 2011.

[8] I. Husain and M. Ehsani, "Torque ripple minimization in switched reluctance motor drives by PWM current control," *IEEE Transactions on Power Electronics*, vol. 11, no. 1, pp. 83–88, 1996.

[9] H. Cheng, "Adaptive variable angle control in switched reluctance motor drives for electric vehicle applications," *Journal of Power Electronics*, vol. 17, p. 1512, 2017.

[10] M. Rodrigues, P. J. Costa Branco, and W. Suemitsu, "Fuzzy logic torque ripple reduction by turn-off angle compensation for switched reluctance motors," *IEEE Transactions on Industrial Electronics*, vol. 48, no. 3, pp. 711–715, 2001.

[11] R. P. Krishna, "Efficiency improvement and torque ripple minimisation of four-phase switched reluctance motor drive using new direct torque control strategy," *IET Electric Power Applications*, vol. 14, p. 52, 2020.

[12] K. J. Hoon and K. R. Young, "Sensorless direct torque control using the inductance inflection point for a switched reluctance motor," *IEEE Transactions on Industrial Electronics*, vol. 65, p. 52, 2018.

[13] R. H. Seung, "Torque ripple minimization scheme using torque sharing function based fuzzy logic control for a switched reluctance motor," *Journal of Electrical Engineering and Technology*, vol. 10, p. 118, 2015.

[14] J. Ye, B. Bilgin, and A. Emadi, "An offline torque sharing function for torque ripple reduction in switched reluctance motor drives," *IEEE Transactions on Energy Conversion*, vol. 30, no. 2, pp. 726–735, 2015.

[15] C.-H. Lin, "Adaptive nonlinear backstepping control using mended recurrent Romanovski polynomials neural network and mended particle swarm optimization for switched reluctance motor drive system," *Transactions of the Institute of Measurement and Control*, vol. 41, no. 14, pp. 4114–4128, 2019.

[16] C.-L. Tseng, S.-Y. Wang, S.-C. Chien, and C.-Y. Chang, "Development of a self-tuning TSK-fuzzy speed control strategy for switched reluctance motor," *IEEE Transactions on Power Electronics*, vol. 27, no. 4, pp. 2141–2152, 2012.

[17] Z. Lin, D. S. Reay, B. W. Williams, and X. He, "Online modeling for switched reluctance motors using B-Spline neural networks," *IEEE Transactions on Industrial Electronics*, vol. 54, no. 6, pp. 3317–3322, 2007.

[18] A. Anand and B. Singh, "Design and implementation of PFC Cuk converter fed SRM drive," *IET Power Electronics*, vol. 10, no. 12, pp. 1539–1549, 2017.

[19] A. Anand and B. Singh, "PFC-based half-bridge dual-output converter-fed four-phase SRM drive," *IET Electric Power Applications*, vol. 12, no. 2, pp. 281–291, 2018.

[20] S. Muthulakshmi and R. Dhanasekaran, "A new front end capacitive converter fed switched reluctance motor for torque ripple minimization," *Circuits and Systems*, vol. 7, no. 5, pp. 585–595, 2016.

[21] J. Chai, "On the switched-reluctance motor drive with three-phase single-switch switch-mode rectifier front-end," *IEEE Transactions on Power Electronics*, vol. 25, p. 1135, 2010.

[22] J.-W. Ahn and D.-H. Lee, "Performance of passive boost switched reluctance converter for single-phase switched reluctance motor," *Journal of Electrical Engineering and Technology*, vol. 6, no. 4, pp. 505–512, 2011.

[23] C. Zhang, K. Wang, S. Zhang, X. Zhu, and L. Quan, "Analysis of variable voltage gain power converter for switched reluctance motor," *IEEE Transactions on Applied Superconductivity*, vol. 26, no. 7, pp. 1–5, 2016.

[24] D. Panda and V. Ramanarayanan, "Reduced acoustic noise variable DC-bus-voltage-based sensorless switched reluctance motor drive for HVAC applications," *IEEE Transactions on Industrial Electronics*, vol. 54, no. 4, pp. 2065–2078, 2007.

[25] J. Reinert and S. Schroder, "Power-factor correction for switched reluctance drives," *IEEE Transactions on Industrial Electronics*, vol. 49, no. 1, pp. 54–57, 2002.

[26] M. Mohamadi, A. Rashidi, S. M. S. Nejad, and M. Ebrahimi, "A switched reluctance motor drive based on quasi Z-source converter with voltage regulation and power factor correction," *IEEE Transactions on Industrial Electronics*, vol. 65, no. 10, pp. 8330–8339, 2018.

[27] A. Anand and B. Singh, "Modified dual output cuk converter-fed switched reluctance motor drive with power factor correction," *IEEE Transactions on Power Electronics*, vol. 34, no. 1, pp. 624–635, 2019.

[28] H. Vasquez and J. K. Parker, "A new simplified mathematical model for a switched reluctance motor in a variable speed pumping application," *Mechatronics*, vol. 14, no. 9, pp. 1055–1068, 2004.

[29] M. Y. Ma, "Subsection PWM variable duty cycle control of switched reluctance motor based on current soft chopping," *Proceedings of the Chinese Society of Electrical Engineering*, vol. 38, p. 5582, 2018.

[30] K. Hirachi and M. Nakaoka, "Improved control strategy on single-phase buck-type power factor correction converter," *International Journal of Electronics*, vol. 86, no. 10, pp. 1281–1293, 1999.

[31] S. Shin, N. Kawagoe, T. Kosaka, and N. Matsui, "Study on commutation control method for reducing noise and vibration in SRM," *IEEE Transactions on Industry Applications*, vol. 54, no. 5, pp. 4415–4424, 2018.

[32] C.-Y. Wu and C. Pollock, "Analysis and reduction of vibration and acoustic noise in the switched reluctance drive," *IEEE Transactions on Industry Applications*, vol. 31, no. 1, pp. 91–98, 1995.

[33] R. Ali, "Investigation of optimal control for vibration and noise reduction in-wheel switched reluctance motor used in electric vehicle," *Mathematics and Computers in Simulation*, vol. 167, p. 267, 2020.